Nanostructure of EVA/Organoclay Nanocomposites: Effects of Kinds of Organoclays and Grafting of Maleic Anhydride onto EVA

Xiucuo Li, [1] **Chang-Sik Ha**[2]

[1]*School of Chemical Engineering, Hebei University of Technology, Tianjin 300130, China*
[2]*Department of Polymer Science and Engineering, Pusan National University, Pusan 609-735, Korea*

Received 3 January 2002; accepted 11 July 2002

ABSTRACT: Nanostructure of poly(ethylene-*co*-vinyl acetate)/organically modified montmorillonite (MMT; EVA/organoclay) nanocomposites prepared by melt intercalation process was investigated using X-ray diffraction (XRD) and transmission electron microscopy (TEM). Three kinds of organoclays were used to see their influences on the nanostructure of the EVA hybrids. The effects of the polar interactions between the polymer and the silicate layers of organoclays were also investigated by grafting maleic anhydride onto EVA. It was found that the strong polar interactions between the polymer and the silicate layers of organoclays are critical to the formation of polymer-layered silicate nanocomposites. The results also showed that increasing the mixing temperature was unfavorable to improve the dispersion of organoclays in the EVA matrix. J Appl Polym Sci 87: 1901–1909, 2003

Key words: ethylene–vinyl acetate copolymer; organically modified montmorillonite; nanocomposites; melt intercalation; nanostructure

INTRODUCTION

Montmorillonite (MMT) is a kind of clay consisting of stacked silicate layers with a basal spacing of around 1 nm. The silicate layer is separated from its neighbors by a Van der Waals gap called gallery, which is occupied by hydrated alkaline or alkaline-earth metal cations. By replacing the metal cations with onium such as alkylammonium cation through ion exchange reaction, the hydrophilic MMT is rendered hydrophobic or organophilic, which makes it possible for the polymers with varying polarity to intercalate in, forming polymer-layered silicate (PLS) nanocomposites.[1,2]

Two kinds of PLS nanocomposites can be obtained depending on the nature of the components used (layered silicate, organic cation, and polymer) and the preparation method.[3] In intercalated PLS nanocomposites, the polymer chain is intercalated between the silicate layers, resulting in a well-ordered multilayer morphology with alternating polymeric and silicate layers (a basal spacing larger than that of the original MMT or organically modified MMT, i.e., organoclay). When the silicate layers are completely delaminated into nanometer-sized single layers, which are dispersed uniformly in the polymer matrix, an exfoliated or delaminated PLS nanocomposite is obtained.

To prepare PLS nanocomposites, four main processes can be used: solution intercalation, in situ intercalative polymerization, polymer melt intercalation, and template synthesis. Polymer melt intercalation is appealing and well-studied because of its versatility, its compatibility with current polymer processing techniques, and its environmentally benign character. So far, many polymers have been studied as a base polymer for PLS nanocomposites through melt intercalation process, including nylon,[4,5] polystyrene,[6–8] polypropylene,[9–12] silicone rubber,[13] ethylene–vinyl acetate copolymer (EVA),[3,14,15] poly(butylene terephtalate),[16] and poly(ethylene oxide).[17] They exhibit improved properties, including modulus, thermal stability, solvent resistance, enhanced ionic conductivity, flame retardancy, and so on.

The thermodynamics that drives the melt intercalation of a polymer into an organic layered silicate has been studied by several groups.[18–22] Unfortunately, however, there are still no generally applicable guidelines as to optimum polymer-layered silicate combination. Consequently, in PLS nanocomposites, synthesis is currently a tedious trial-and-error process.

In this work, we prepared EVA/organoclay nanocomposites by melt intercalation process. Zanetti et al.[14] and Alexandre et al.[3,15] also prepared EVA/organic layered silicate nanocomposites by melt intercalation method. Alexandre and Dubois[3] found that nanocomposites were only formed when EVA was

Correspondence to: Chang-Sik Ha (csha@pnu.edu).
Contract grant sponsor: the Brain Korea 21 Project in 2001.
Contract grant sponsor: the Center of Integrated Molecular Systems, POSTECH, Korea.

TABLE I
Structural Information of Different Kinds of Organoclays

Organoclay	Ammonium cation	XRD peak position (2θ)	Basal spacing (001)
Cloisite 6A	$(CH_3)_2$ $(HT)_2N^+$	2.49°, 4.72°	3.57 nm
Closite 10A	$(CH_3)_2$ $(HT)(CH_2C_6H_5)N^+$	4.52°	2.00 nm
Cloisite 30B	(CH_3) $(T)(CH_2CH_2OH)_2N^+$	4.73°	1.88 nm

T = tallow (~65% C18, ~30% C16, ~5% C14); HT = hydrogenated tallow.

melt-blended at 130°C with nonfunctionalized organo-MMT, such as MMT exchanged with dimethyldioctadecyl ammonium. Zanetti et al.[14] prepared EVA nanocomposites with fluorohectorite-like synthetic silicate exchanged with octadecylammonium and studied their thermal behaviors. In the present work, three kinds of organoclays, each possessing different ammonium cations, were selected in order to investigate their influences on the nanostructure of the EVA hybrids. Additionally, EVA was also grafted with maleic anhydride (MAH) in order to investigate the effects of polar interactions on the nanocomposite formation.

EXPERIMENTAL

Materials

EVA with vinyl acetate content of 18 mol % was obtained from Du Pont (Elvax 460; melt flow index = 2.5 g/10 min; melt flow index based on ASTM D 1238, 190°C, 2.16 kg). Maleic anhydride (MAH) was purchased from Aldrich Chemical. Dicumyl peroxide (DCP) with purity >98% was used as an initiator for the grafting of MAH onto EVA. Its half-life time at 175°C was about 1.45 min. The organoclays were supplied by Southern Clay Products under the trade names of Cloisite 6A, Cloisite 10A, and Cloisite 30B. Table I and Figure 1 give the related structure information and the X-ray diffraction (XRD) patterns, respectively, of each of the organoclays.

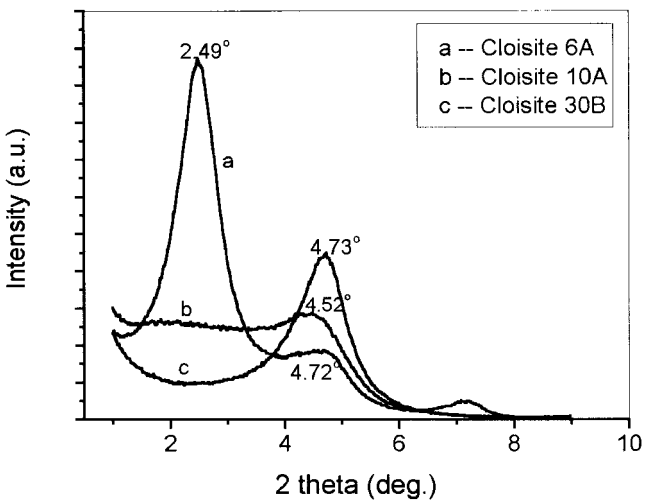

Figure 1 The XRD patterns of three kinds of organoclays.

Melt grafting of MAH onto EVA

EVA was dried at 80°C under vacuum for at least 10 h before use. MAH was grafted onto the EVA in a Haake Rheocord mixer at 175°C, 50 rpm, based on the same conditions used by Kim et al.[23] The reaction time was 10 min.

Preparation of EVA/organoclay hybrids

The organoclays and the EVA pellets were dried under vacuum at 80°C for at least 10 h before use. EVA was mixed with 3 wt % of organoclays in an internal mixer (Haake Rheocord Mixer) for 15 min. The rotor speed was 50 rpm and the temperature was set at 140°C, unless otherwise specified. In the case of the MAH-grafted EVA (EVA-*g*-MAH), the mixing temperature was set at 175°C, mixing time 20 min. The mixed product was injection-molded using a CS-183 MMX mini MAX molder (Custom Scientific Instruments) to get bulk samples for XRD and transmission electron microscopy (TEM) characterization.

Characterization

X-ray diffraction studies of the samples were carried out using a Rigaku D/max 2200H X-ray diffractometer (40 kV, 50 mA) at a scanning rate of 0.5°/min. TEM images were taken from cryogenically microtomed ultrathin sections using a Hitachi H-800 TEM.

RESULTS AND DISCUSSION

Dispersion of organoclays in EVA matrix

To investigate the effects of kinds of organoclays on the nanostructure of EVA hybrids, we selected three organoclays, Cloisite 6A, Cloisite 10A, and Cloisite 30B. They have different hydrophobicity due to the existence of different ammonium cations located in the silicate galleries. Figure 2 shows the XRD patterns of the EVA/organoclay hybrids containing 3 wt % of organoclays. It is obvious that the structure of the hybrids depends on the organoclay used. In contrast

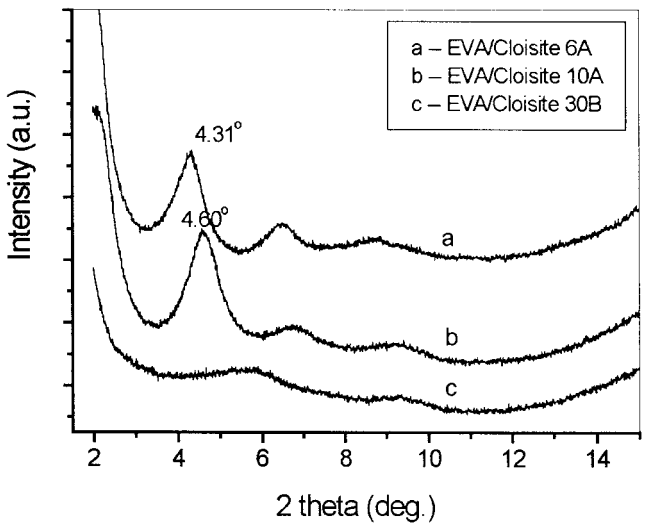

Figure 2 XRD patterns of the EVA/organoclay hybrids containing 3 wt % of organoclay.

to the Cloisite 6A, the EVA/Cloisite 6A hybrid shows no peak at 2.49°, and the peak at 4.72° has shifted to 4.31°, indicating the intercalated and even partially exfoliated hybrid structure. The XRD pattern of the EVA/Cloisite 30B hybrid shows almost no peak, meaning a high degree of intercalation with layer spacings higher than 4–5 nm and/or exfoliation of the silicate layers in the EVA matrix. For the EVA/Cloisite 10A hybrid, the original peak of the Cloisite 10A at about 4.6° still remains, but a new peak trace is observed at about 2°, indicating only partially intercalated structure of the EVA/Cloisite 6A hybrid.

To confirm the nanostructure of the EVA/organoclay hybrids and verify the conclusions from XRD, TEM studies at varying magnifications were carried out. In Figure 3, TEM images with low magnification of 20 K (those with 500 nm of scale bar) show that the size of the dispersed particles decreases in the sequence of Cloisite 10A, 6A, and 30B. The primary particles of Cloisite 6A have been delaminated into crystallites with several silicate layers, which are uniformly dispersed in the EVA matrix. The disappearance of the peak at 2.49° should originate from the partial exfoliation of the silicate layers and too large basal spacing to be detected in the present 2θ range. There are still some of the crystallites, which show clearly several silicate layers with a basal spacing corresponding to the XRD peak at 4.31°.

Two kinds of dispersed silicate particles exist in the TEM image of the EVA/Cloisite 10A hybrid as shown in Figure 3(b). One is with large agglomerates present and shows no intercalation, with almost the same basal spacing of around 2.0 nm as the original Cloisite 10A. The other is smaller in size and exhibits an intercalated structure corresponding to the peak at around 2°. For the EVA/Cloisite 30B hybrid, the silicate layers have been exfoliated, even though the silicate particles are not uniformly dispersed in the EVA matrix as nanometer-sized single layers [Fig. 3(c)]. In this way, the 001 reflection was not observed in its XRD pattern.

In general, the outcome of polymer melt intercalation is determined by the interplay of entropic and enthalpic factors.[18] The confinement of the polymer chains inside the silicate galleries results in a decrease in the overall entropy of the polymer chains, and the increased conformational freedom of the tethered ammonium cations compensates the entropy loss as the silicate layers separate with each other. However, the small increase in the gallery spacing does not influence the total entropy change; rather, the total enthalpy will drive the intercalation. The enthalpy of mixing has been classified into two components: the interaction between polymer and ammonium cations and the interaction between the layered polar silicates and the polymer chains. In most conventional organomodified silicates, the tethered ammonium cations are apolar. The apolar interactions between the polymer and ammonium cations are unfavorable to the polymer melt intercalation. In such cases, the enthalpy of mixing can be rendered favorable by the establishment of polar polymer–silicate surface interactions.

The above theoretical concepts can be used to explain the results of the EVA/organoclay hybrids. With two bulky tallow groups, the ammonium cations present in the Cloisite 6A are the most hydrophobic. The biggest initial gallery spacing (ca. 3.57 nm) and the related weak interaction between the silicate layers of Cloisite 6A allow for easier intercalation of the EVA chains. The consequent expansion of the gallery and especially the partial exfoliation of the silicate layers compensate the entropy loss of the chain intercalation by the freedom of ammonium cations. On the other hand, the polar interactions between the carboxyl group of EVA and the silicate layers are necessary to drive the intercalation of EVA chains and partial exfoliation of the silicate layers. In this sense, the failure of polypropylene (PP) and low density polyethylene (LDPE) to form nanocomposites with organoclays was reported to be in part due to the lack of polar interactions between the apolar polymer and the silicate layers.[12]

In contrast to the Cloisite 6A, the ammonium cations in Cloisite 30B contain two hydroxyethyl groups. The driving force of the intercalation and exfoliation for the EVA/Cloisite 30B hybrid should originate from the strong polar interaction between the carboxyl groups present in EVA and hydroxyl groups of the ammonium cations.

The hydrophobicity of the Cloisite 10A is in between those of the Cloisite 6A and the Cloisite 30B. In comparison to the Cloisite 30B, there are no strong polar interactions between EVA and ammonium cations of the Cloisite 10A, and the interlayer spacing of the Cloisite 10A is smaller than that of the Cloisite 30B.

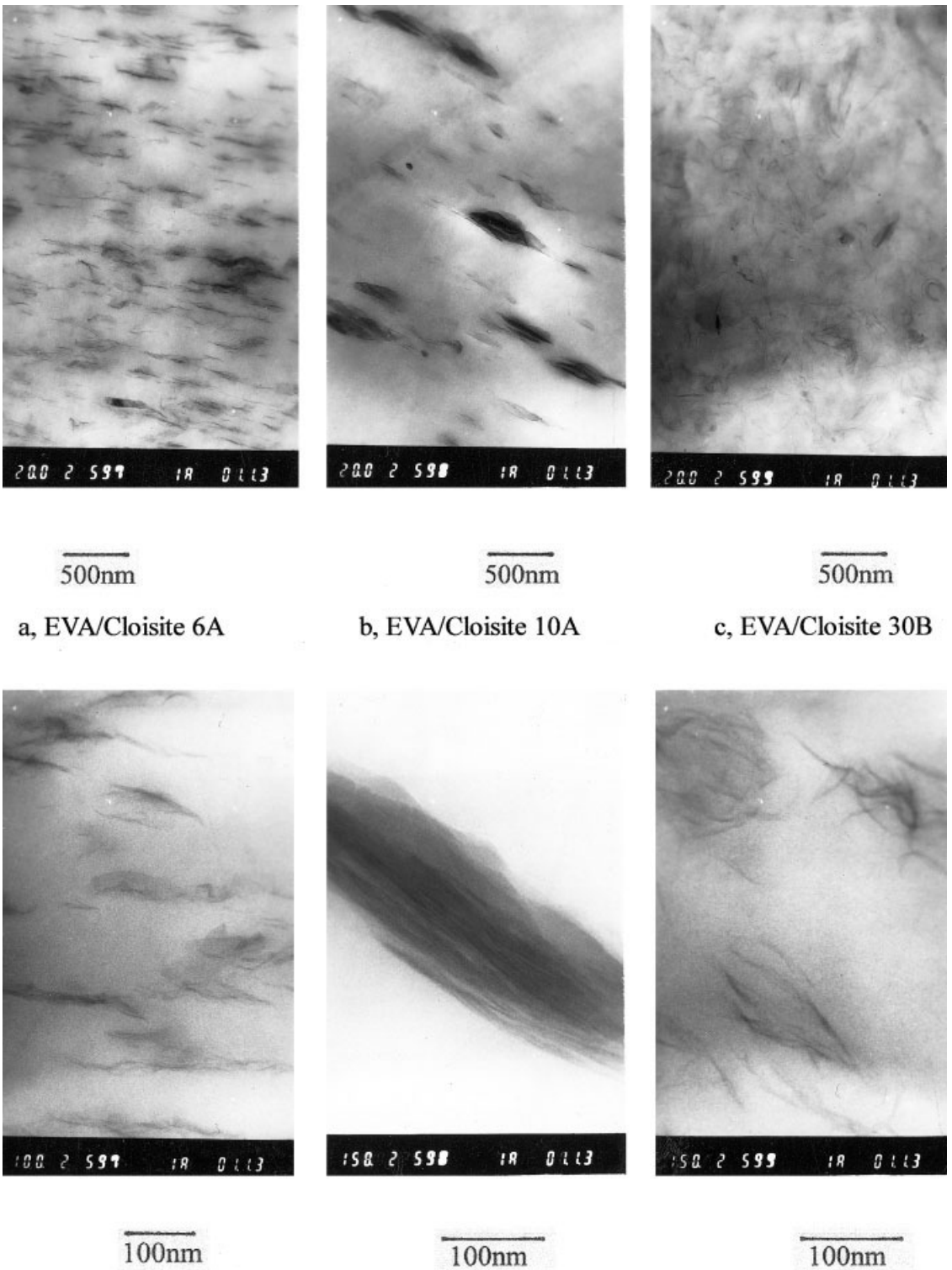

Figure 3 TEM images of the EVA/organoclay hybrids at different magnifications.

Thus, it is difficult for the EVA chains to intercalate into the galleries of Cloisite 10A, and EVA can form only partially intercalated hybrids with Cloisite 10A.

Nanostructure of EVA-*g*-MAH/organoclay hybrids

To investigate the influence of strong polar interactions between polymer and organoclays on the nanostructure of PLS nanocomposites, EVA was grafted with 2phr (wt) MAH (the detailed reaction mechanism of EVA-*g*-MAH was disclosed in our previous study[23]). The grafted EVA (EVA-*g*-MAH) was then mixed with 3 wt % of organically modified MMT in the Rheocord Mixer at 175°C for 20 min. The EVA-*g*-MAH/organoclay hybrids were characterized by XRD

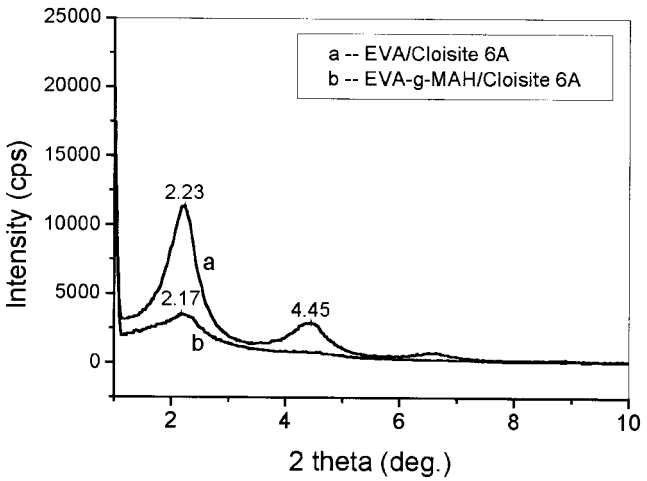

Figure 4 XRD patterns of the EVA/Cloisite 6A and the EVA-*g*-MAH/Cloisite 6A hybrids containing 3 wt % of Cloisite 6A.

and TEM, together with the comparison of EVA/organoclay hybrids prepared at the same processing conditions.

Figures 4 and 5 show the XRD patterns and TEM micrographs of the EVA-*g*-MAH/Cloisite 6A and the EVA/Cloisite 6A hybrids, respectively. It is seen that the dispersion states of the Cloisite 6A in the EVA-*g*-MAH matrix become much better than those in the EVA matrix. The original peaks of the Cloisite 6A at around 2.49° and 4.72° have shifted to 2.23° and 4.45°, respectively, indicating an intercalated structure of the EVA/Cloisite 6A hybrid. There are some large agglomerates present in the TEM image with low magnification, but the one with high magnification shows clearly the layered structure of the larger particles, which are intercalated with the polymer. However, the XRD pattern of the EVA-*g*-MAH /Cloisite 6A hybrid (Fig. 4) exhibits only one relatively weak peaks at lower 2θ of 2.17°. Therefore, the Cloisite 6A layers in the EVA-*g*-MAH matrix should be expected to intercalate with high degree and even partially exfoliated. The TEM images in Figure 5 show that most of the silicate layers of the Cloisite 6A have been exfoliated and dispersed uniformly in the EVA-*g*-MAH matrix, though a slight amount of unexfoliated layers exist. The existence of the weak peak in the XRD pattern should be attributed to these unexfoliated layers.

For the EVA/Cloisite 10A hybrid, the dispersion states of the Cloisite 10A in the EVA matrix have also been greatly improved by using the EVA-*g*-MAH instead of the EVA in the matrix as shown in Figures 6 and 7. The existence of the original peak of the Cloisite 10A at around 4.6° suggests no intercalation, while the new peak at around 1.96° indicates the intercalation of EVA in the galleries of the Cloisite 10A. Thus, the EVA/Cloisite 10A hybrid exhibits only a partially intercalated nanostructure. The TEM images confirm the above XRD results by showing partial intercalation by EVA with large particles of Cloisite 10A present. On the other hand, the EVA-*g*-MAH/Cloisite 10A hybrid exhibits a relatively small shoulder around 2.82°, with a gradual increase in the XRD strength toward low angle (Fig. 6). Completely exfoliated and dispersed PLS hybrids such as the nylon–clay hybrid exhibit no peak, but instead display a gradual increase in the diffraction intensity toward low diffraction angles.[24] Therefore, the silicate layers of the Cloisite 10A in the EVA-*g*-MAH matrix should be exfoliated and well dispersed. This is confirmed by the TEM images showing the homogeneous dispersion of completely

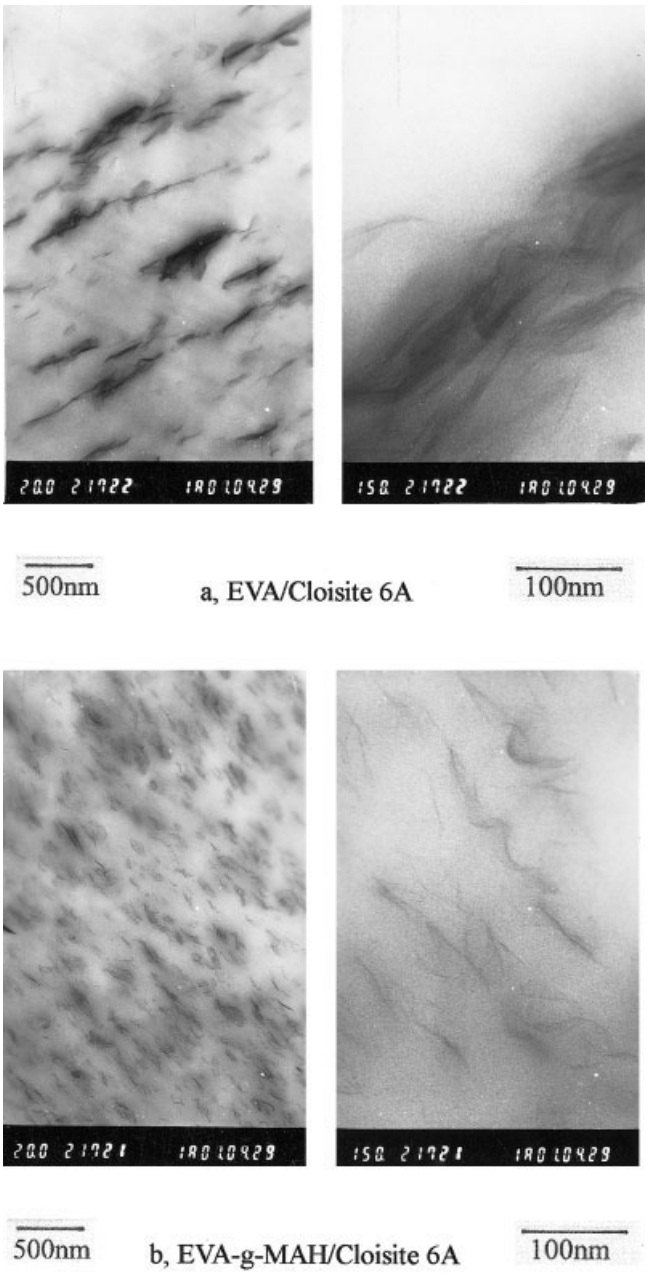

Figure 5 TEM images of the EVA/Cloisite 6A and the EVA-*g*-MAH/Cloisite 6A hybrids.

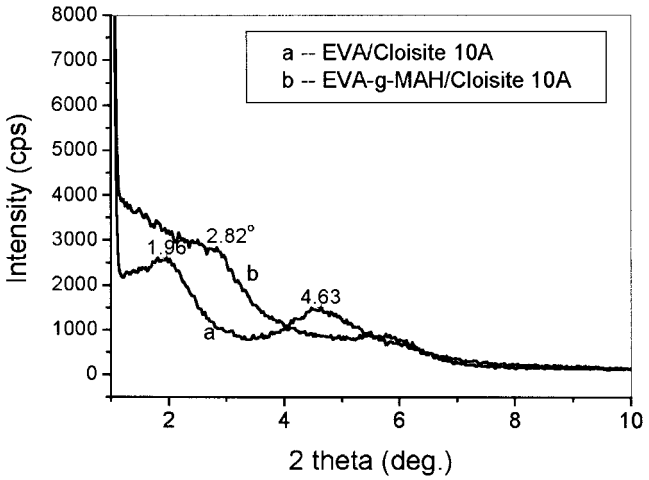

Figure 6 XRD patterns of the EVA/Cloisite 10A and the EVA-*g*-MAH/Cloisite 10A hybrids containing 3 wt % of Cloisite 10A.

delaminated single silicate layers in the EVA-*g*-MAH matrix, as shown in Figure 7(b).

The influence of the grafting of MAH onto EVA on the nanostructure of the EVA/Cloisite 30B hybrid is quite different from that of the EVA/Cloisite 6A and the EVA/Cloisite 10A hybrids. Even though its XRD pattern exhibits only a weak peak at 4.42° (Fig. 8), the TEM image with low magnification in Figure 9(b) shows no uniformity, with very big Cloisite 30B agglomerates dispersed in the EVA-*g*-MAH matrix. Rather, the EVA/Cloisite 30B hybrid exhibits more uniform dispersion of the silicate layers intercalated and partially exfoliated in the EVA matrix, as shown in the XRD and TEM results. This further confirms that TEM is necessary to determine the nature of the polymer–clay hybrids and to provide additional information, especially when XRD data exhibit featureless diffraction patterns.[8] XRD and TEM have been regarded as complementary in characterizing the nanostructure of the PLS nanocomposites.

The variable influences of the grafting of MAH onto EVA on the dispersion states of organoclays in the polymer matrix can be interpreted based on the polymer melt intercalation thermodynamics. As mentioned above, the strong polar interactions between the polymer and organoclays are critical to the formation of intercalated and especially exfoliated nanocomposites. The driving force for the formation of mostly exfoliated EVA-*g*-MAH/Cloisite 6A nanocomposite and completely exfoliated EVA-*g*-MAH/Cloisite 10A nanocomposite originates from the strong hydrogen bonding between the MAH group (or —COOH group generated from the hydrolysis of the MAH group) and the oxygen groups or hydroxyl groups of the silicates. Other researchers found similar results in preparing PLS nanocomposites.[11,19,25,26]

At present, it is more difficult to explain why the use of EVA-*g*-MAH degrades the dispersion of Cloisite 30B. The ammonium cations present in the Cloisite 30B are the most hydrophilic with their two hydroxyethyl groups. Grafting EVA with MAH gives EVA higher polarity to be able to match with that of the Cloisite 30B, which in turn favors an intercalation. But the result is quite the opposite. The existence of MAH groups along the EVA chains may disrupt the optimum combination of EVA with Cloisite 30B, or too strong polymer–organic silicate layer interactions may increase the frictional coefficient associated with poly-

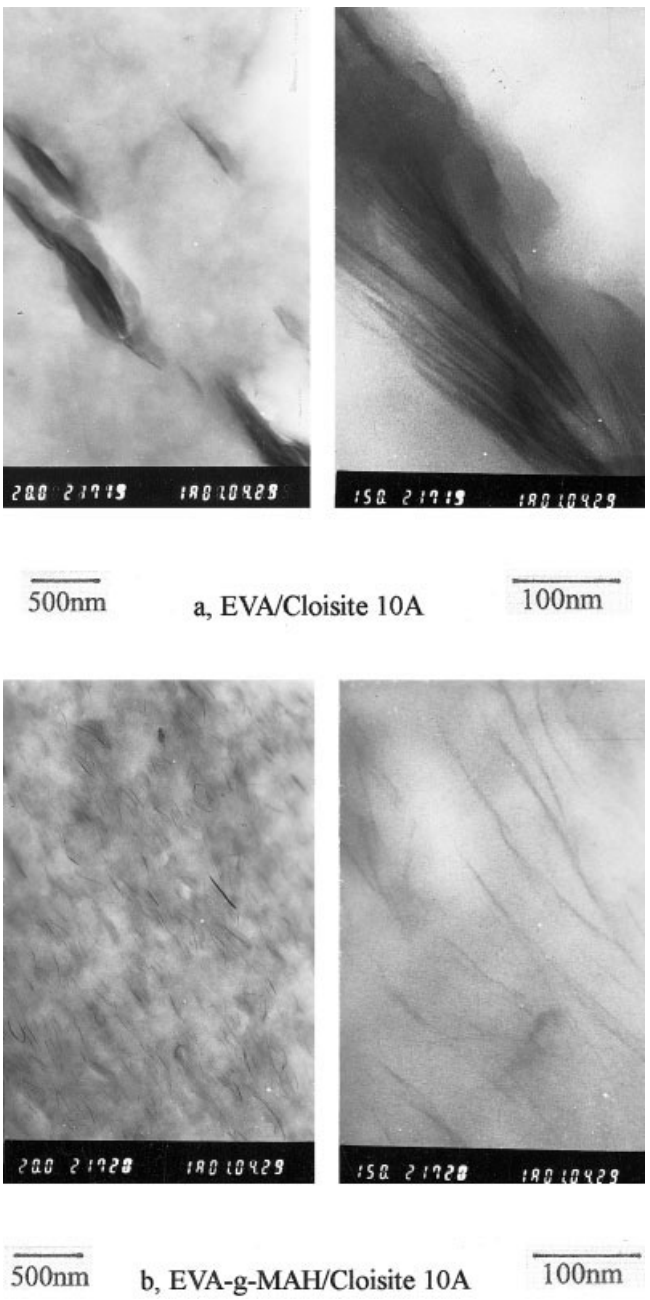

Figure 7 TEM images of the EVA/Cloisite 10A and the EVA-*g*-MAH/Cloisite 10A hybrids.

mer transport within the interlayer and result in slower melt intercalation kinetics.[8] More detailed research is under way to dig out the reason and the mechanism of the above process.

Influence of mixing temperature on nanostructure of EVA/organoclay hybrids

Comparing the TEM micrographs of Figure 3(a) with Figure 5(a), Figure 3(b) with Figure 7(a), and Figure 3(c) with Figure 9(a), one can see the influences of the mixing temperature on the nanostructure of EVA/organoclay hybrids. According to the kinetics of polymer melt intercalation,[27] the increasing temperature leads to higher polymer diffusion rates, thus favoring the hybrid formation. Vaia and Giannelis[18] found similar results in the preparation of polystyrene nanocomposites, in which higher anneal temperatures favor the hybrid formation. However, for EVA/organoclay hybrids, it is obvious that the high mixing temperature (175°C) is unfavorable for well-dispersed PLS nanocomposites; even though the mixing time is 5 min longer at 175°C than that at 140°C, EVA/organoclay hybrids prepared at 175°C still show worse dispersion state of the organoclays in the EVA matrix as shown in the TEM micrographs. The XRD patterns further confirm the above results if one compares the curves of Figure 2 (line a) with Figure 4 (line a), Figure 2 (line b) with Figure 6 (line a), and Figure 2 (line c) with Figure 8 (line a).

To confirm the above results, EVA/Cloisite 30B nanocomposites were prepared at the same processing conditions, only at different temperatures. Figures 10 and 11 represent the XRD patterns and the TEM images of the prepared hybrids, respectively. The XRD patterns of the EVA/Cloisite 30B hybrids in Figure 10 show that the hybrids prepared at low temperatures

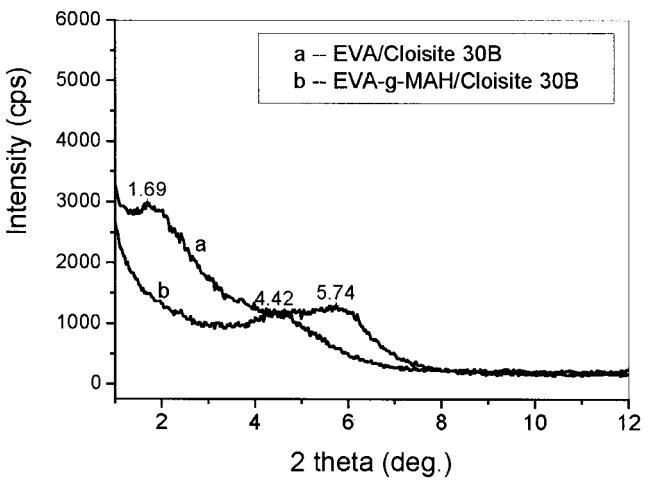

Figure 8 XRD patterns of the EVA/Cloisite 10A and the EVA-*g*-MAH/Cloisite 30B hybrids containing 3 wt % of Cloisite 30B.

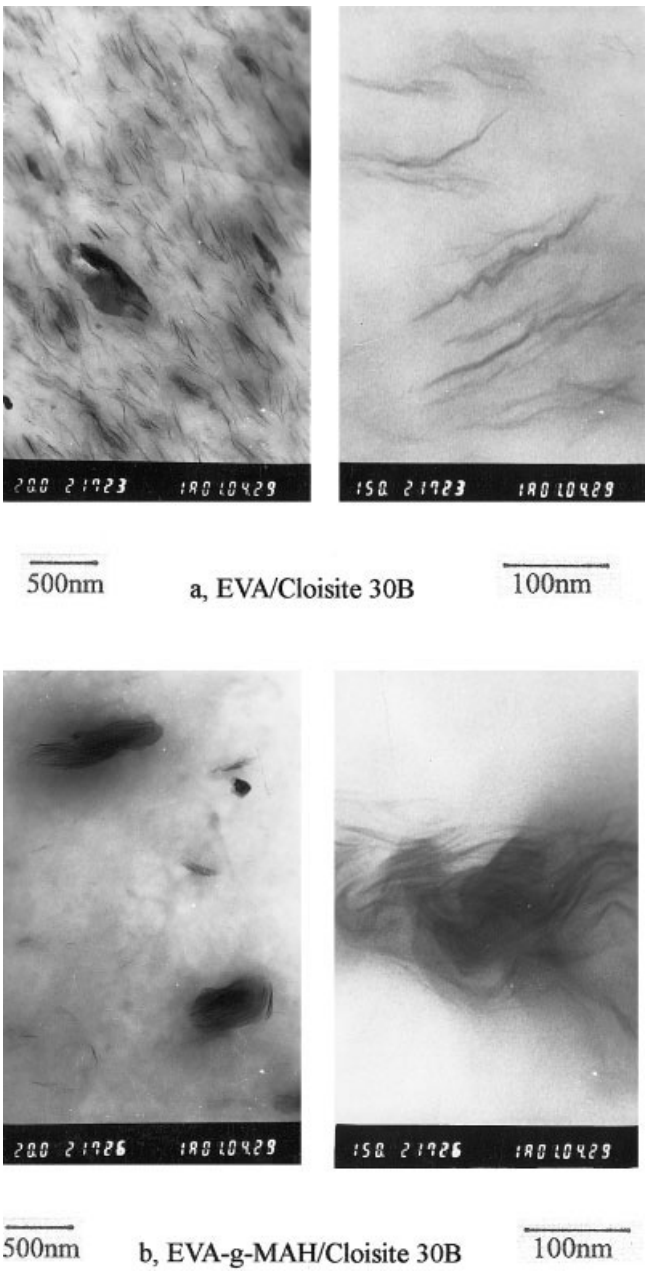

Figure 9 TEM images of the EVA/Cloisite 30B and the EVA-*g*-MAH/Cloisite 30B hybrids.

such as 130°C and 140°C show almost no peaks (Fig. 10, lines a and b), indicating low degree of intercalation and/or exfoliation of the Cloisite 30B silicate layers in the EVA matrix. The corresponding TEM images in Figures 11(a) and 3(c) indicate that the exfoliated silicate layers of Cloisite 30B dispersed more uniformly when prepared at 130°C. On the other hand, the hybrid prepared at high temperature, 175°C, exhibits a weak peak around 6° in the XRD pattern, and less uniform dispersion of the silicate particles in the EVA matrix with a few large particles as shown in the TEM images of Figure 11(b). Thus, we conclude that better dispersion states of Cloisite 30B in the EVA

matrix were obtained at lower mixing temperature (130°C).

The main reason for the above observations can be explained based on the effect of an external shear on the formation of polymer/organoclay nanocomposites via melt intercalation process. The presence of an externally applied shear would promote the exfoliation of the silicate layers.[27] Huh and Balaz[28] also found that the polymer–clay mixture can readily form an exfoliated nanocomposites under shear, which can remove the bridging force between the two confining silicate layers. If the mixing temperature is lower, the torque or the shear will be higher in preparation of EVA/organoclay nanocomposites via melt intercalation at constant shear rate. This strong shear is necessary to promote the delamination of the silicate layers in the EVA matrix, due to the proper combination of the external shear and interaction between EVA and the organic silicate layers.

CONCLUSIONS

The nanostructure of the EVA/organoclay nanocomposites prepared via the polymer melt intercalation process have been investigated here. The dispersion of the organoclays in the EVA matrix depends on the hydrophobicity of the organoclays and especially the polar interactions between the silicate layers and EVA chains. For the strong hydrogen-bonding interactions between EVA and Cloisite 30B, the EVA/Cloisite 30B nanocomposite shows mostly exfoliated structure, while the EVA/Cloisite 10A hybrid can only possess a partially intercalated structure due to the lack of strong polar interactions and entropy compensation by the freedom of ammonium cations. By introducing the strong hydrogen bonding to the EVA/organoclay hybrids through grafting MAH onto EVA, the dispersion states of EVA/organoclay hybrids were greatly improved for both Cloisite 6A and Cloisite 10A hybrid systems. In the EVA-*g*-MAH/Cloisite 10A nanocomposite, a complete exfoliation was observed, whereas in the EVA-*g*-MAH/Cloisite 6A hybrid mostly exfoliated morphology was observed. It was concluded that both hybrids show much better dispersion of organoclays in the EVA-*g*-MAH matrix than the corresponding EVA/organoclay hybrids. It was difficult, however, to explain the different influences of the grafting MAH onto EVA on the dispersion of Cloisite 30B in the EVA matrix.

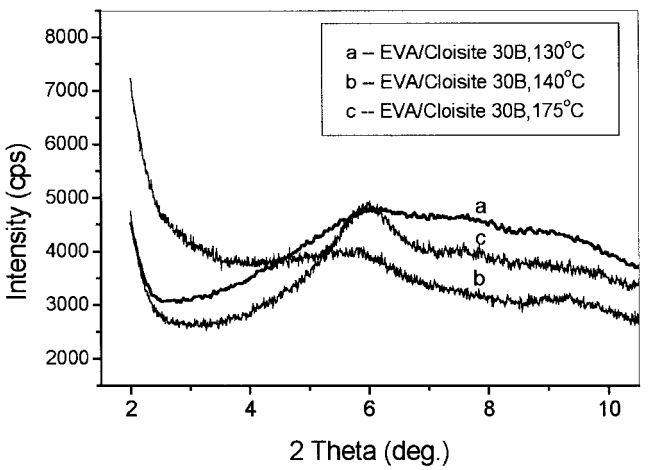

Figure 10 XRD patterns of the EVA/Cloisite 30B hybrids containing 3 wt % of Cloisite 30B prepared at different temperatures.

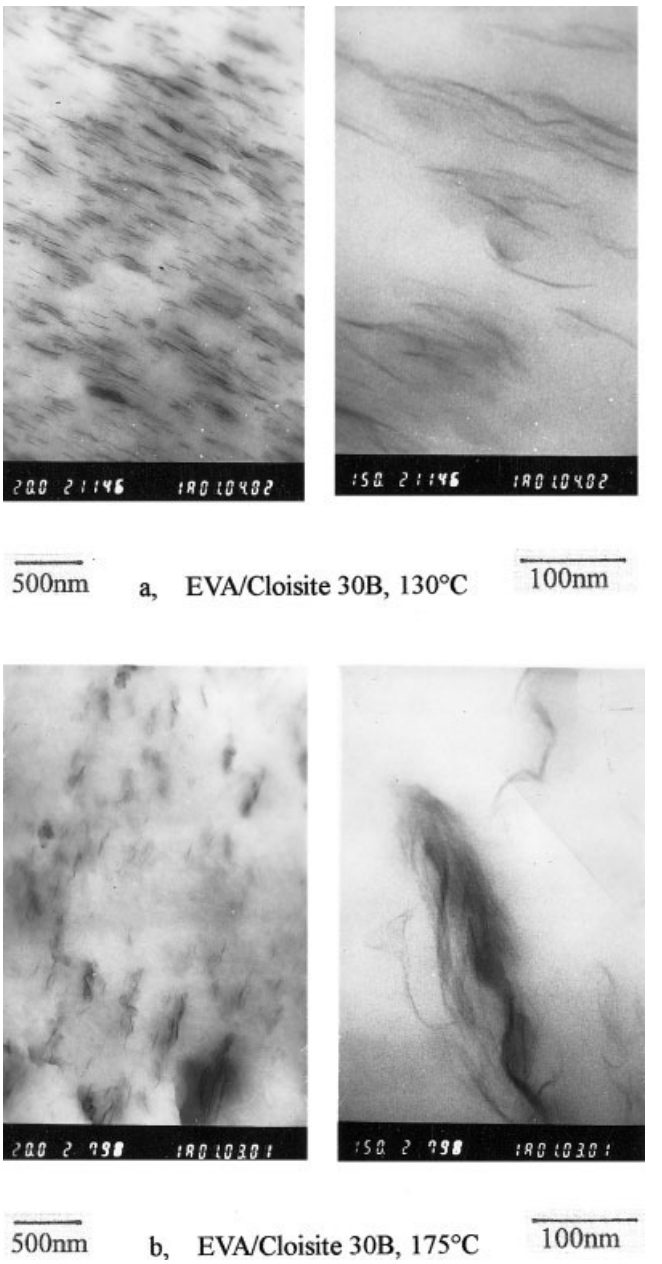

Figure 11 TEM images of the EVA/Cloisite 30B hybrids containing 3 wt % of Cloisite 30B prepared at different temperatures.

The dispersion state of organoclays in the matrix became worse with increasing the mixing temperature of EVA with organoclays, probably due to the decreased external shear at high temperatures, as the external shear is necessary for the nanocomposite formation.

The authors thank Mr. C. Z. Kim and H. M. Park for their helps in preparing samples with Haake Rheocorder Mixer.

References

1. Zanetti, M.; Lomakin, S.; Camino, G. Macromol Mater Eng 2000, 279, 1.
2. Lebarn, P. C.; Wang, Z.; Pinnavaia, T. J. Appl Clay Sci 1999, 15, 11.
3. Alexandre, M.; Dubois, P. Mater Sci Eng 2000, 28, 1.
4. Kim, G.-M.; Lee, D.-H.; Hoffmann, B.; Kressler, J.; Stöppelmann, G. Polymer 2001, 42, 1095.
5. Cho, J. W.; Paul, D. R. Polymer 2001, 42, 1083.
6. Xu, X.; Qutubuddin, S. Polymer 2001, 42, 807.
7. Chen, G.M.; Liu, S. H.; Zhang, S. F.; Qi, Z. N. Macromol Rapid Commun 2001, 21, 746.
8. Vaia, R. A.; Jandt, K. D.; Giannelis, E. P. Chem Mater 1996, 8, 2628.
9. Reichert, P.; Nitz, H.; Klinke, S.; Brandsch, R.; Thomann, R.; Mulhaupt, R. Macromol Mater Eng 2000, 275, 8.
10. Galgali, G.; Ramesh, C.; Lele, A. Macromolecules 2001, 34, 852.
11. Kawasumi, M.; Hasegawa, N.; Kato, M.; Usuki, A.; Okada, A. Macromolecules 1997, 30, 6333.
12. Usuki, A.; Kato, M.; Okada, A.; Kurauchi, T. J. J Appl Polym Sci 1997, 63, 137.
13. Burnside, S. D.; Giannelis, E. P. Chem Mater 1995, 7, 1597.
14. Zanetti, M.; Camino, G.; Thomann, R.; Miilhaupt, R. Polymer 2001, 42, 4501.
15. Alexandre, M.; Beyer, G.; Henrist, C.; Cloots, R.; Rulmont, A.; Jerome, R.; Dubois, R. Macromol Rapid Commun 2001, 22, 643.
16. Li, X.; Kang, T.; Cho, W.J.; Lee, J.K.; Ha, C.S. Macromol Rapid Commun 2001, 22, 1310.
17. Chen, W.; Xu, Q.; Yuan, R. Z. Mater Sci Eng 2000, B77, 15.
18. Vaia, R. A.; Giannelis, E. P. Macromolecules 1997, 30, 7990.
19. Vaia, R. A.; Giannelis, E. P. Macromolecules 1997, 30, 8000.
20. Balazs, A. C.; Singh, C.; Zhulina, E. Macromolecules 1998, 31, 8370.
21. Balazs, A. C.; Singh, C.; Zhulina, E. ACC Chem Res 1999, 8, 651.
22. Lyatskata, Y.; Balazs, A. C. Macromolecules 1998, 31, 6676.
23. Kim, S.-J.; Shin, B.-S.; Hong, J.-L.; Cho, W.-J.; Ha, C.-S. Polymer 2001, 42, 4073.
24. Usuki, A.; Kawasumi, Y.; Kojima, M.; Fukushima, Y.; Okada, A.; Kurauchi, T.; Kamigaito, O. J Mater Res 1993, 8, 1179.
25. Ishida, H.; Campbell, S.; Blackwell, J. Chem Mater 2000, 12, 1260.
26. Yoon, J. T.; Jo, W. H.; Lee, M. S.; Ko, M. B. Polymer 2001, 42, 329.
27. Vaia, R. A.; Jandt, K. O.; Kramer, E. J. Giannelis, E. P. Macromolecules 1995, 28, 8080.
28. Huh, J.; Balazs, A. C. Polym Mater Sci Eng 1999, 81, 449.